DOI: 10.13009/EUCASS2017-502

Calculated and experimental binary phase diagrams for ADN and AN based solid propellants – H2020 GRAIL project

Xavier Sécordel, Dimitri Daigurande,* Romain Beauchet,* Yann Batonneau,* Charles Kappenstein* and Niklas Wingborg***

**Institut de Chimie des Milieux et Matériaux de Poitiers (IC2MP)*
CNRS – UMR7285, Université de Poitiers, 4 rue Michel Brunet, bâtiment B27, TSA 51106, Poitiers cedex 9, France
***Swedish Defence Research Agency, FOI*
Department of Energetic Materials, SE-147 25 Tumba Sweden

Abstract

In the frame of the European H2020 project GRAIL [1], a green oxidizer couple, ammonium dinitramide (ADN, $[NH_4]^+[N(NO_2)_2]^-$) and ammonium nitrate (AN, $[NH_4]^+[NO_3]^-$), is considered as an alternative to ammonium perchlorate (AP, $[NH_4]^+[ClO_4]^-$).
In this context, the binary ADN-AN phase diagram calculation was performed using a basic model based on ideal ionic liquid and pure non miscible solid phases and compared to the experimental phase diagram determined by DSC analyses of twenty-four prepared compositions. These results are supplemented by estimated binary phase diagrams of AP-ADN and AP-AN systems.

1. Introduction

The knowledge of phase diagrams is a key parameter for the formulation of solid propellants, in particular for the oxidizer content. In the frame of the European H2020 project GRAIL [1], the well-known ammonium perchlorate (AP, $[NH_4]^+[ClO_4]^-$) is proposed to be replaced by ammonium dinitramide (ADN, $[NH_4]^+[N(NO_2)_2]^-$) and ammonium nitrate (AN, $[NH_4]^+[NO_3]^-$) in order to circumvent both health issues of AP and the formation of considerable amounts of hydrochloric acid released subsequently to its decomposition.
Both oxidant have their ammonium cations in common ($[NH_4^+]$) and possess anions composed of oxygen and nitrogen atoms. To the best of our knowledge, no binary diagram of the ADN-AN mixture have been proposed in open literature so far. Only a crude sketch, as mentioned by Rahm [2] of ADN-AN is proposed. The latter was drawn from the melting temperatures of the respective compounds and a result reported in a study by Pavlov *et al.* [3]. However, only the temperature (60 °C) and the composition of the eutectic are given in this work but no precision on the determination method, calculated and/or experimental, is included. The composition of AN-ADN mixture is announced to be AN:ADN = 1:2. Rahm might have considered the same value (with a probable confusion between ADN and AN as the composition drawn on the binary diagram corresponds to AN:ADN = 2:1) [2]. The composition proposed seems to be a molar composition and thus corresponds to a molar ratio of x_{ADN} = 0.67. Furthermore, Russel *et al.* [4] give the eutectic point at 55 °C for a mixture with a molar ratio of x_{ADN} = 0.7 which is in good agreement with the value given by Pavlov *et al.*[3]. Finally, among ADN-AN mixtures with different ratios analysed using differential scanning calorimetry (DSC) by Ziru *et al.* [5], the maximum endotherm is obtained for a mixture with x_{ADN} =0.71 demonstrating that the eutectic point is close to this value.
As only little information on the binary ADN-AN phase diagram can be found in the open literature, this paper presents the results of calculation which was performed using a simple model based on ideal ionic liquid and pure non miscible solid phases. The same model was used for AN-AP and ADN-AP mixtures. Further, DSC analyses were carried out on numerous ADN-AN mixtures with different molar ratio in order to verify and refine the predicted binary diagram.

DOI: 10.13009/EUCASS2017-502

2. Calculation model

For the three binary diagrams, ADN-AN, ADN-AP and AN-AP, calculations were performed to determine the liquidus spots using the equation dedicated to the freezing point depression [6]:
Two assumptions are made to calculate this diagram: (i) total immiscibility of solids whatever the mixture composition, and (ii) liquidus profile modelized by straight lines which cross each other at the eutectic point. The following equation was thus used to estimate the liquidus frontiers:

$$\Delta T = \left(\frac{R\,T^{*2}}{\Delta_{fus}H}\right) \times x(B), \text{leading to: } T = -\left(\frac{R\,T^{*2}}{\Delta_{fus}H}\right) \times x(B) + T^{*} \qquad (1)$$

with : T^*: melting point of compound B (°C)
T: Liquidus temperature (°C)
x(B): Mole fraction of the compound B
$\Delta_{fus}H$: Enthalpy of fusion of compound B

Table 1 gathers the enthalpy of fusion and the melting temperature of ADN [7], AN [8] and AP [9] needed to apply this model.

Table 1: enthalpy of fusion and melting points of ADN, AN, and AP

	$\Delta_{fus}H$ / kJ mol^{-1}	T_{fus} / °C
ADN	17.62	92.9
AN	6.11	169.6
AP	29.30	240

3. Experimental procedure

The ammonium dinitramide used for this study was a prilled ADN from Eurenco Bofors AB. The ammonium nitrate was supplied by Yara AB.
Both products were ground separately in air in an agate mortar and then sieved in order to obtain grains with diameter between 40 and 100 µm. The powders weare then dried at 50 °C for 12 to 14 h at the end of the working day before the preparation of the mixtures.
The preparation of the ADN-AN mixtures (200 mg) was carried out in a glove box under an argon atmosphere. They were introduced into 4 mL vials. Powders were then mixed with a spatula for 1 min after shaking by hand. This protocol was repeated before the mixtures were introduced into the DSC crucibles. The crucibles were sealed with a press out of the glove box.
DSC analysis tests were carried out using a TA Instuments model DSC Q20 apparatus of ADN-AN mixtures under 50 mL min^{-1} of N_2 with a heating rate of 2 °C min^{-1} from ambient temperature to a temperature above the decomposition temperature of the mixture.
Cycling DSC tests of ADN-AN mixtures were carried out under 50 mL min^{-1} of N_2 with the following cycle: from 2 °C min^{-1} heating ramp to 110 °C followed by a 2 °C min^{-1} cooling ramp down to 25 °C. The cycle is repeated twice.
Compositions of the mixtures and sample mass analyzed using DSC are presented in Table 2.

DOI: 10.13009/EUCASS2017-502

Table 2: Composition and mass of the ADN-AN samples analysed

ADN targeted molar fraction	Mass (g)		Molar fraction (-)		Sample mass analysed (mg)
	ADN	AN	ADN	AN	
0.000	-	0.2000	0	1	2.6
0.016	0.0050	0.1952	0.016	0.984	2.3
0.033	0.0099	0.1900	0.0325	0.9675	3.9
0.050	0.0150	0.1853	0.05	0.9504	2.9
0.067	0.0210	0.1807	0.0697	0.9303	2.7
0.139	0.0399	0.1601	0.1384	0.8616	2.4
0.217	0.0599	0.1411	0.2149	0.7851	2.4
0.301	0.0800	0.1200	0.301	0.699	2.3
0.345	0.0900	0.1101	0.345	0.655	2.3
0.392	0.1000	0.1000	0.392	0.608	2.3
0.424	0.1064	0.0933	0.424	0.576	2.0
0.458	0.1133	0.0869	0.457	0.543	3.6
0.492	0.1199	0.0810	0.4883	0.5117	2.4
0.545	0.1300	0.0699	0.545	0.455	2.0
0.601	0.1399	0.0599	0.601	0.399	2.6
0.721	0.1600	0.0408	0.717	0.283	2.2
0.750	0.1643	0.0354	0.75	0.25	2.7
0.853	0.1800	0.0205	0.85	0.15	3.4
0.888	0.1851	0.0149	0.889	0.111	2.2
0.925	0.0950	0.0050	0.925	0.075	3.0
0.962	0.1949	0.0051	0.961	0.039	2.1
0.981	0.1974	0.0025	0.981	0.019	2.6
1	0.2000	-	1	-	2.8

4. Results and discussion

4.1 Calculated diagram

Calculated liquidus points with the method mentioned previously are shown in Figure 1. Both straight lines, corresponding to the liquidus frontier for ADN on the right and for AN on the left, have been drawn. The intersection gives the eutectic point which allows estimating the position of the eutectic point. In the case of ADN-AN mixture, the estimated eutectic point is at 54.9 °C for a mol fraction of ADN x_{ADN} = 0.43.

AN is known to have multiple solid-solid transition phases before melting. Usually and above 0 °C, the IV→III transition occurs at 32 °C, the III→II transition at 84 °C and finally the II→I one at 125 °C [10]. Therefore, these phase transitions are added to the calculated liquidus and deduced solidus into the diagram.

DOI: 10.13009/EUCASS2017-502

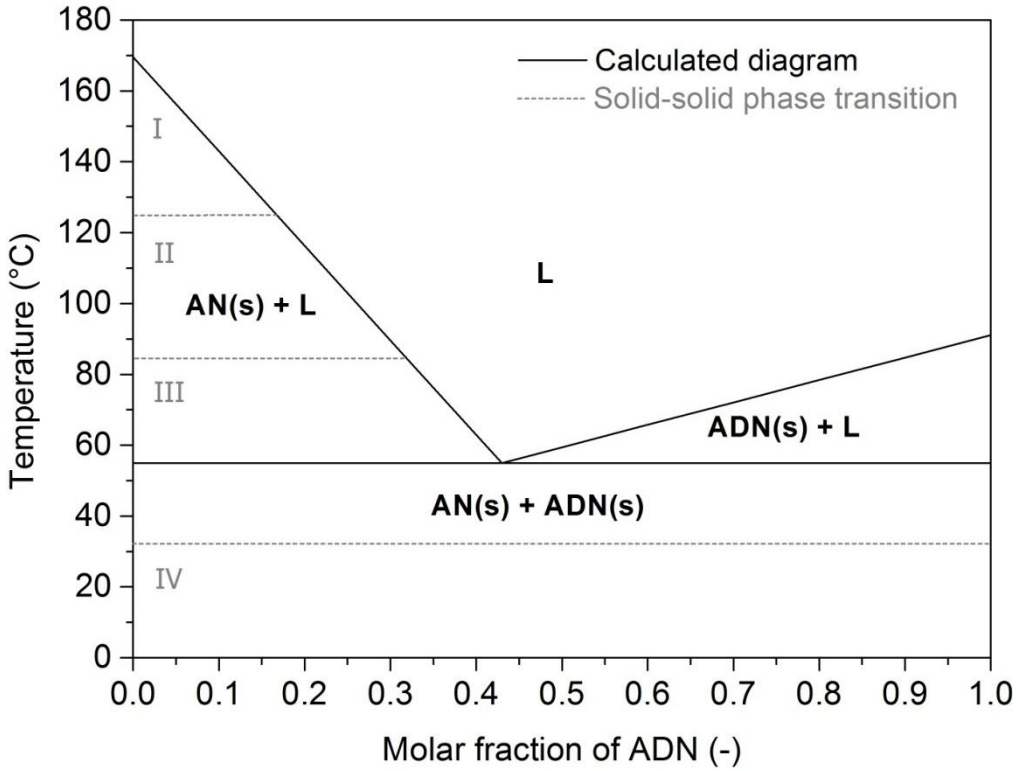

Figure 1: ADN-AN calculated binary diagram at 1 bar. Crystal phases of AN are delimited by horizontal, dashed lines

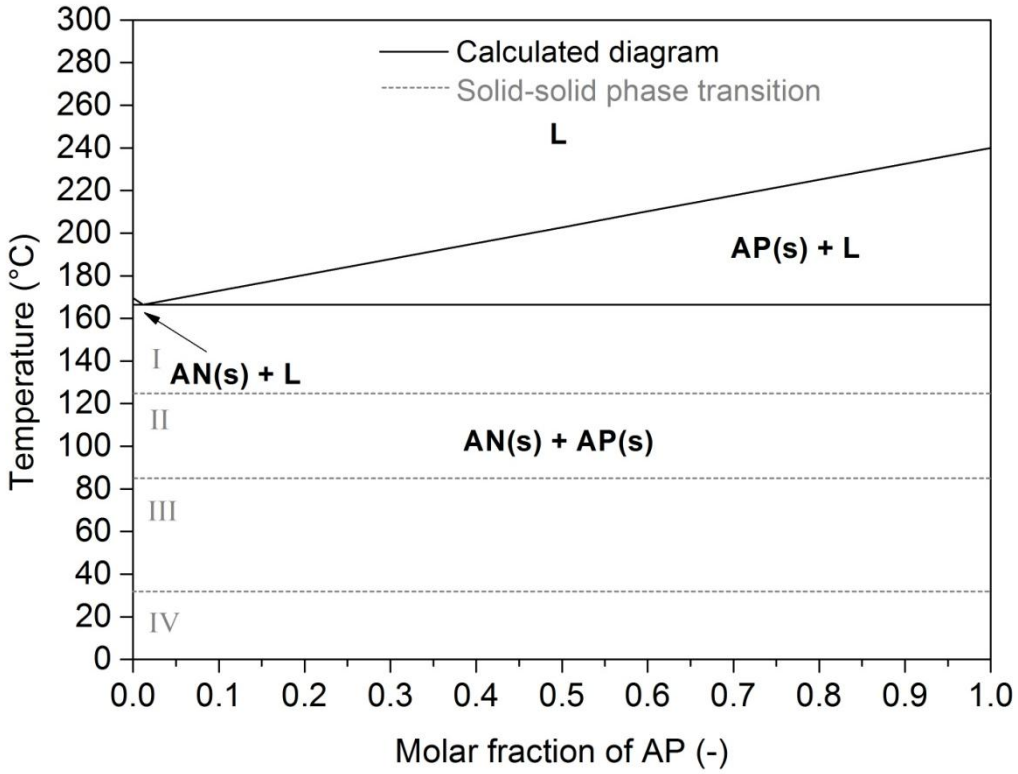

Figure 2: AN-AP calculated binary diagram at 1 bar. Crystal phases of AN are delimited by horizontal, dashed lines

DOI: 10.13009/EUCASS2017-502

In the case of AN-AP, the eutectic point seems to be situated at very low molar ratio of AP, being x_{AP} = 0.01, and at a temperature close to the melting point of AN which seems to be close to 166.4 °C. Thus, the eutectic line can be drawn at 166.4 °C.

The tentative drawing of the calculated binary diagram of ADN-AP shows the limit of this simple model to propose a binary diagram. The important gap between the melting points of these two compounds shows that a eutectic is unlikely. However, a peritectic point could be observed in this particular case.

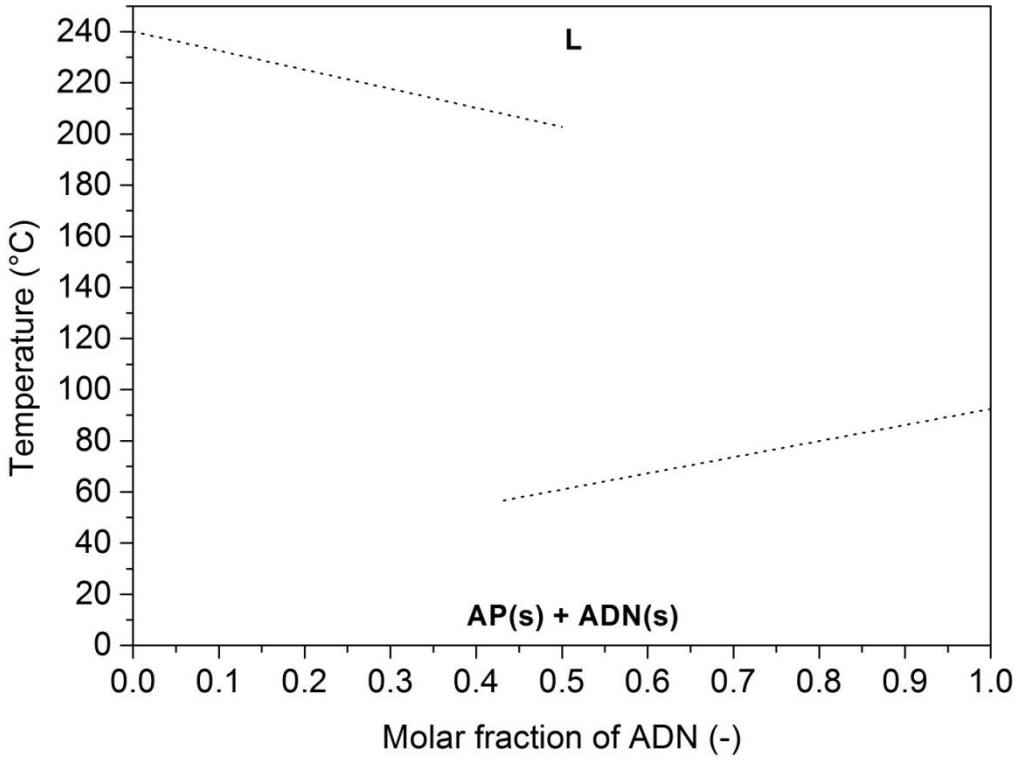

Figure 3: ADN-AP calculated binary diagram at 1 bar

4.2 Experimental binary diagram

DSC analyses results of the pure compounds are displayed in Figure 4 and Figure 5. Results for ADN show a melting temperature onset at 90.5°C and a melting endotherm minimum at 91.7 °C. The corresponding energy is equal to 182.6 J g^{-1} (22.9 kJ mol^{-1}), which is slightly above the literature data (17.4 [7] and 17.62 kJ mol^{-1} [11]).

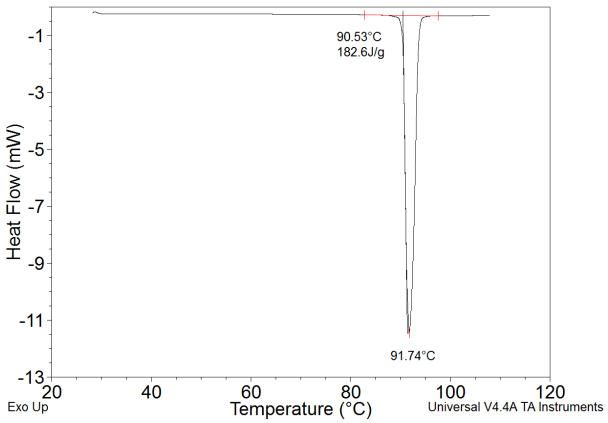

Figure 4 : DSC analysis of pure ADN

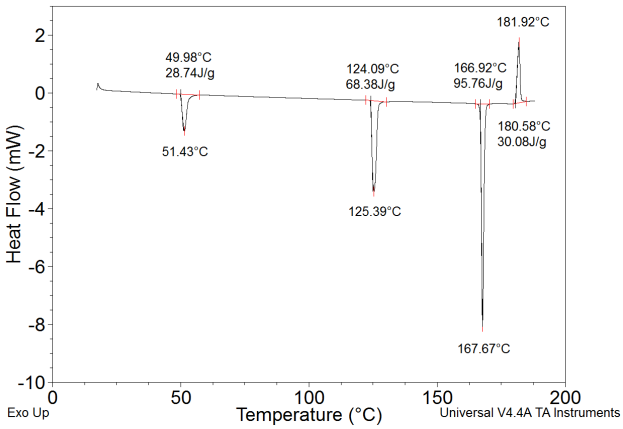

Figure 5 : DSC analysis of pure AN

DOI: 10.13009/EUCASS2017-502

As mentioned before, usually, three phase transitions are observed above 0 °C at 32, 84 and 125 °C. DSC analysis of pure AN does not show the presence of the endothermic peak corresponding to the III →II phase transition (expected at *ca.* 84 °C). A second analysis of another sample of the same AN was carried out and led to the same result. This could be explained, as reported by W. Engel and K. Menke, to the absence of water [10]. When AN is sufficiently dried the IV→III and III →II transitions are merged by bypassing phase III. This results in a IV→ II transition at around 45 °C. Figure 5 shows that this transition takes place at 50 °C. The next endothermic event is assigned to the II→I solid transition at 124 °C while the last endothermic peak is related to the melting of the material at 167 °C. The enthalpy of fusion value as deduced from the experiment is 7.6 kJ mol^{-1} whereas literature mentions 6.1 kJ mol^{-1} [8] and 6.4 kJ mol^{-1} [12]. Values are quite close to each other. Finally, an exothermic peak at 182 °C is observed, being the evidence of a very slight decomposition process (2.4 kJ mol^{-1}). This event is unusual and could probably be explained either by a reaction with the crucible either in the presence of trace of impurities both catalysing the decomposition.

Cycling DSC analysis test was carried out with an ADN-AN mixture of 92.5/7.5 mol-% and is shown in Figure 6. The endothermic melting peak of ADN is observed during the first heating ramp. However, no recrystallisation is observed during the temperature decrease as no exothermic peak can be detected. After analysis, the closed crucible was weighed and the mass was identical to that before analysis, showing no mass loss. A second test was conducted under the same conditions with a 75/25 mol % ADN/AN mixture and is displayed in Figure 7. As observed in the previous test, no recrystallisation peak could be detected during the first cooling phase. It seems that the kinetic of crystallisation (including supercooling issues) is too slow in these operating conditions so that the use of a cycling method remains inappropriate to determine the liquidus point.

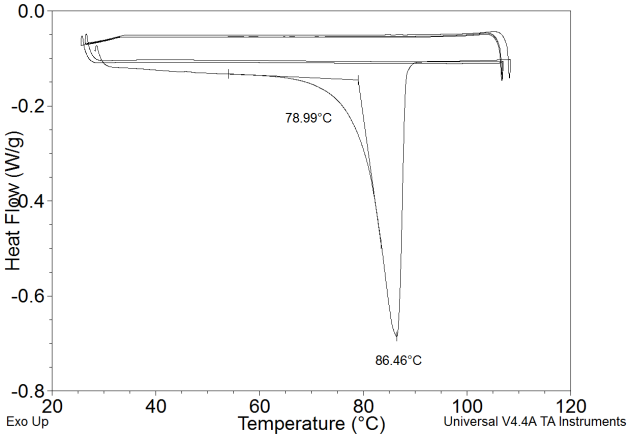

Figure 6: Cycling DSC of ADN-AN mixture (92.5/7.5 mol %)

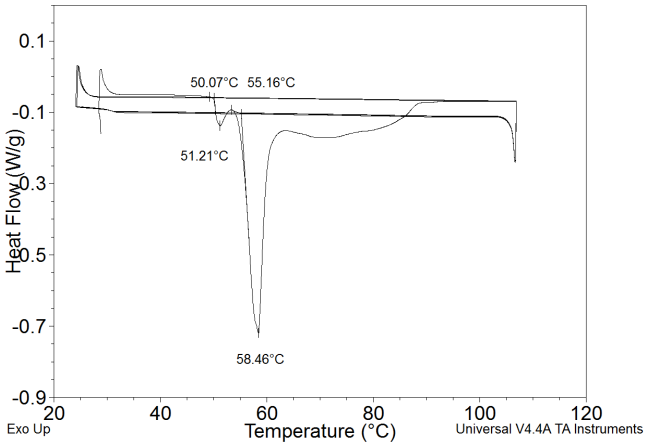

Figure 7: Cycling DSC of ADN-AN mixture (75/25 mol %)

Next tests were consequently programmed by running one single heating ramp of 2 °C min^{-1}. Analyzes were stopped before (for samples with $x_{ADN} > 0.350$) and at the beginning (for samples with $x_{ADN} < 0.350$) ADN decomposition.

DSC analyses of pure compounds and mixtures are reported in Figure 8 and the resulting data extracted are listed in Table 3 and Table 4. From $x_{ADN} = 0.000$, two clear endothermic peaks appear close to 52 and 126 °C, corresponding to the IV→II and II→I solid-solid transitions, respectively. The II→I transition peak integrated intensity decreases progressively when increasing amount of ADN and vanishes for $x_{ADN} = 0.2170$. The peak surfaces lead to the values 68.38 J g^{-1} for pure AN to 1.846 J g^{-1} for $x_{ADN} = 0.2170$. A very tiny peak appears at about 85 °C when ADN is added and could be attributed to the III→II AN phase transition. The observation of this band could be due to the release of water by ADN. This peak also decreases with increasing molar ratio of ADN and seems to disappear at 0.301.
The new peak close to 60 °C is typical of the eutectic transition at constant temperature; as expected, its surface increase, then decreases when the ADN content overpasses the eutectic composition. Further, the temperature and surface of both melting peaks decrease from pure component to mixtures, in agreement with a classical binary phase diagram.

DOI: 10.13009/EUCASS2017-502

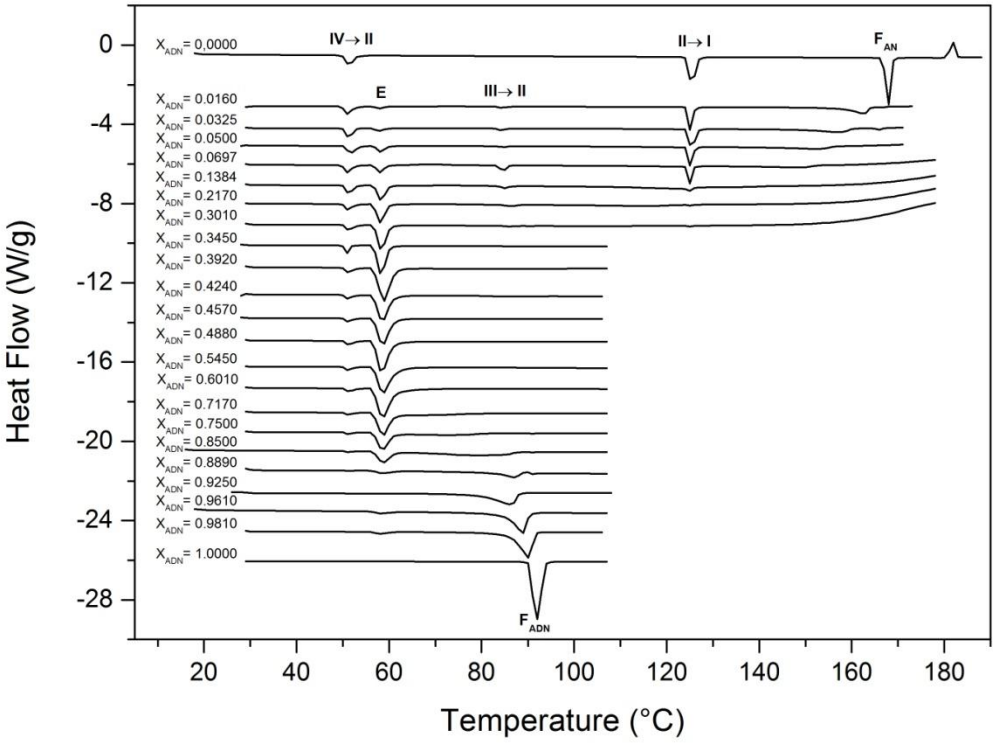

Figure 8: DSC analyses of the pure compounds and of ADN-AN mixtures. Values given correspond to mol fraction of ADN in the mixture

Melting of ADN and AN can be both observed in the mixture for $x_{ADN} > 0.8700$ and $x_{ADN} < 0.0697$ respectively. The difficulty to observe or to measure precisely the melting of the compounds in the $0.0697 < x_{ADN} < 0.8700$ range could come either from the ease of ADN thermal decomposition in the solid state in the presence of AN [2], [5], and/or from the overlapping of the endotherm with solid-solid phase transition; this is the case for $x_{ADN} = 0.1384$, from the broadening of the endotherms, or any combination of these phenomena. For these reasons, the value of melting temperature for ADN and AN reported in Table 3 at 0.7500 and 0.2170, respectively, need to be carefully considered. In this work, the thermal decomposition of ADN was measured at 136 °C.

DOI: 10.13009/EUCASS2017-502

Table 3: T_{onset} and T_{max} of the phase transitions as obtained from DSC analyses of different ADN-AN mixtures

x_{ADN}		IV → II	Eutectic	III → II	ADN melting	Peak ~ 91 °C	II → I	AN melting
0.0000	T_{onset}/°C	49.98	-	-	-	-	124.09	166.92
	T_{max}/°C	51.43	-	-	-	-	125.39	167.67
0.0160	T_{onset}/°C	49.80	56.77	83.22	-	-	124.10	159.12
	T_{max}/°C	51.23	58.02	84.46	-	-	124.67	162.81
0.0325	T_{onset}/°C	50.07	56.24	83.15	-	-	124.08	148.86
	T_{max}/°C	51.26	58.12	84.43	-	-	124.81	157.76
0.0500	T_{onset}/°C	50.18	56.74	83.27	-	-	124.10	140.30
	T_{max}/°C	51.91	58.32	84.76	-	-	125.10	152.54
0.0697	T_{onset}/°C	49.82	56.66	83.44	-	-	124.18	134.85
	T_{max}/°C	51.16	58.19	84.7	-	-	124.55	148.29
0.1384	T_{onset}/°C	50.17	56.78	83.69	-	-	>124.16	n.m.
	T_{max}/°C	51.42	58.33	85.21	-	-	124.42	n.m.
0.2170	T_{onset}/°C	49.93	56.63	84.23	-	-	124.19	98.19
	T_{max}/°C	51.33	58.21	86.34	-	-	124.64	116.14
0.3010	T_{onset}/°C	50.25	56.81	84.24	-	90.26	124.26	-
	T_{max}/°C	51.48	58.40	86.39	-	91.09	124.47	-
0.3450	T_{onset}/°C	50.04	56.74	84.19	-	90.01	n.d.	-
	T_{max}/°C	50.68	58.38	86.21	-	90.95	n.d	-
0.3920	T_{onset}/°C	50.04	56.64	84.06	-	89.88	n.d	-
	T_{max}/°C	51.44	59.04	86.90	-	90.76	n.d	-
0.4240	T_{onset}/°C	50.03	56.59	81.90	-	-	n.d	-
	T_{max}/°C	51.25	58.64	82.82	-	-	n.d	-
0.4570	T_{onset}/°C	50.09	56.77					
	T_{max}/°C	51.24	58.56					
0.4880	T_{onset}/°C	50.13	56.67	-	-	n.m.	-	-
	T_{max}/°C	51.49	58.43	-	-	n.m.	-	-
0.5450	T_{onset}/°C	50.06	56.67	-	-	n.m.	-	-
	T_{max}/°C	51.16	58.70	-	-	n.m.	-	-
0.6010	T_{onset}/°C	50.32	56.58	-	-	-	-	-
	T_{max}/°C	51.48	58.84	-	-	-	-	-
0.7170	T_{onset}/°C	50.31	56.62	-	n.m.	88.78	-	-
	T_{max}/°C	51.35	58.94	-	n.m.	90.8	-	-
0.7500	T_{onset}/°C	50.32	56.65	-	64.94	89.95	-	-
	T_{max}/°C	51.19	58.56	-	75.29	90.90	-	-
0.8530	T_{onset}/°C	50.44	56.59	-	n.m.	89.56	-	-
	T_{max}/°C	51.48	58.87	-	n.m.	90.88	-	-
0.8705	T_{onset}/°C	50.39	56.47	-	71.41			
	T_{max}/°C	51.35	58.59	-	81.90			
0.8890	T_{onset}/°C	50.23	56.51	-	82.74	90.37	-	-
	T_{max}/°C	51.15	58.73	-	87.37	90.51	-	-
0.9250	T_{onset}/°C	50.48	56.48	-	80.17	90.37	-	-
	T_{max}/°C	51.10	58.12	-	86.52	90.80	-	-
0.9610	T_{onset}/°C	50.31	56.37	-	85.55	-	-	-
	T_{max}/°C	51.40	58.37	-	89.01	-	-	-
0.9810	T_{onset}/°C	50.47	56.52	-	86.55	-	-	-
	T_{max}/°C	51.39	58.24	-	90.08	-	-	-
1.0000	T_{onset}/°C	-	-	-	90.53	-	-	-
	T_{max}/°C	-	-	-	91.74	-	-	-

n.m : not possible to measure ; n.d : not determined (not analysed)

DOI: 10.13009/EUCASS2017-502

Table 4: DSC peak surface area (in J g^{-1}) during phase transitions for the different mixtures

x_{ADN}	IV → II	Eutectic	III → II	ADN melting	Peak ~ 91 °C	II → I	AN melting
0.0000	28.74	-	-	-	-	68.38	95.76
0.0160	22.63	4.898	3.285	-	-	50.95	52.44
0.0325	23.67	8.614	4.267	-	-	47.71	47.03
0.0500	23.50	16.82	2.342	-	-	40.77	48.78
0.0697	21.98	23.44	13.01	-	-	32.74	32.82
0.1384	22.30	45.44	5.67	-	-	≈11.50.	n.m.
0.2170	17.21	58.66	4.893	-	-	1.846	26.07
0.3010	14.52	82.59	1.723	-	0.1102	1.424	-
0.3450	16.44	95.09	0.4472	-	0.2272	n.d	-
0.3920	11.03	111.3	0.36	-	0.02926	n.d	-
0.4240	11.36	110.3	0.3954	-	-	n.d	-
0.4570	9.410	119.2	-	-	-	-	-
0.4880	11.69	134.6	-	-	n.m.	-	-
0.5450	8.905	136.2	-	-	n.m.	-	-
0.6010	8.420	156.2	-	-	-	-	-
0.7170	5.676	95.16	-	n.m.	0.4361	-	-
0.7500	4.441	69.45	-	18.15	1.013	-	-
0.8530	3.027	48.45	-	n.m.	0.5997	-	-
0.8705	2.339	40.09	-	63.19	-	-	-
0.8890	0.8121	12.15	-	43.46	5.182	-	-
0.9250	1.394	21.53	-	109.1	2.487	-	-
0.9610	0.4332	8.966	-	121.9	-	-	-
0.9810	0.4618	7.492	-	149.7	-	-	-
1.0000	-	-	-	182.36	-	-	-

n.m : not possible to measure ; n.d : not determined (not analysed)

From these data, a tentative experimental binary diagram of the ADN-AN can be proposed. Figure 9 shows the binary diagram plotted from the onset temperatures determined from DSC measurements, Figure 11 represents the binary diagram drawn from the maximum temperatures measured.

DOI: 10.13009/EUCASS2017-502

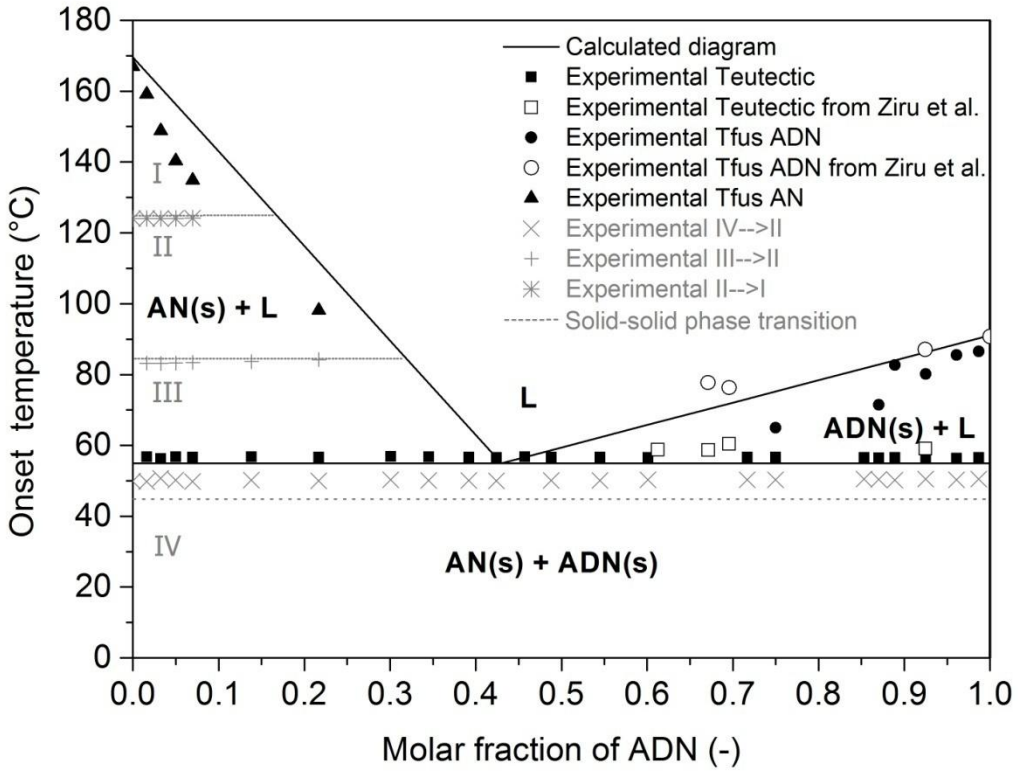

Figure 9: Experimental (with T_{onset}) and calculated binary diagram

Experimental measurement of the solid-solid phase transitions are in quite a good agreement with the calculated ones. The stability in terms of temperature variation of the experimental AN phase transition points both for the III → II and II→I transitions in the AN-rich, univariate region of the diagram seems to account for the low solubility of AN in the liquid phase. The actual observation of the IV→II transition of AN along all the composition axis confirms that the eutectic point is, as expected by the calculation, above 50 °C. For sake of more clarity, the expected IV→III phase transition isotherm was omitted, in Figure 9 and Figure 11, whereas the IV → II transition was superimposed in the form of a grey-dashed line.

The eutectic line calculated at 54.9 °C is close to the experimental plots. However, positions of liquidus points determined experimentally shows that the basic model led to an over-estimation. The experimental plots obtained from Ziru *et al.* [5] were superimposed in Figure 9 and Figure 11. They are close to the calculated points. The liquidus points collected do not allow to estimate and to compare the eutectic point with the calculated one.

However, the variation of the amount of energy absorbed per gram of mixture during eutectic melting as a function of the composition show that a maximum should be reached for a composition of a molar fraction of ADN of 0.6 and thus seems to demonstrate that the eutectic point composition should lie close to this value. This motivated the preparation of Figure 10, in which the aforementioned energy was plotted as a function of the ADN mass fraction to validate this assumption. The expected result in this case is that the energy associated to melting endotherms of the eutectic mixture should increase linearly until the eutectic point and then decrease linearly at higher composition. However, close to the eutectic point, it could be possible to have interference due to the presence of pure compounds and more particularly the superimposition of the endotherm originating from the melting of both the eutectic and the pure compound (due to the low gap of temperatures between the two endotherms). This leads to an anomalous increase of the surface area of the endotherm and thus to a not representative value of the melting of the eutectic mixture quantity. It could be the case, especially on the right side of the eutectic. When ADN-rich mixture gets close to the eutectic point, it becomes difficult to resolve the ADN and the eutectic melting endotherm. Despite this observation, the determination of regression line of points below and above the supposed eutectic point seems to show that two straight lines are obtained with relatively good determination coefficient of about 0.995 and 0.973, and thus, demonstrates that their overlap could be of lower influence than expected when processing the thermal data.

DOI: 10.13009/EUCASS2017-502

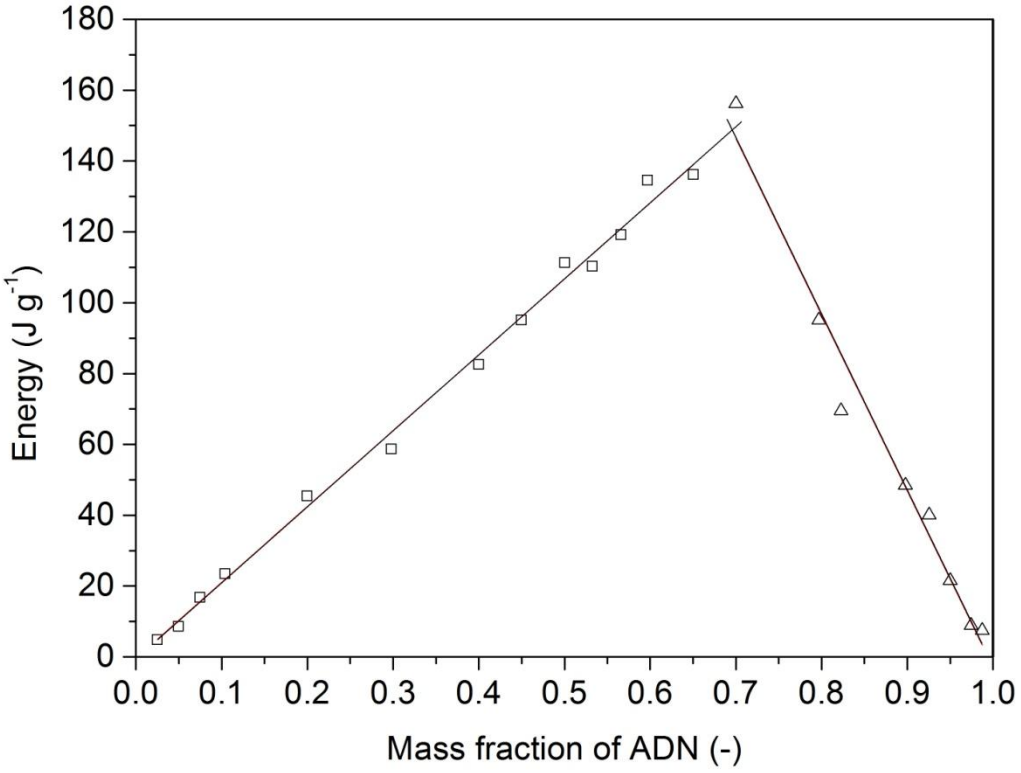

Figure 10: Energy measured by DSC (J g^{-1}) during the melting of the eutectic mixture as a function of the ADN mass fraction.

The results of this estimation gives a eutectic point at a mass fraction w_{ADN} = 0.70 which corresponds to a x_{ADN} = 0.60 at a temperature of about 56.6 °C (onset temperature measured close to x_{ADN} =0.60). This fraction is below the value proposed by Pavlov *et al.* [3] and Russel *et al.* [4] which are respectively equal to x_{ADN} = 0.67 and x_{ADN} = 0.7.

Finally, when plotting the binary phase diagram from the minimum temperature of endotherms, as shown in Figure 11, the points of the liquidus determined experimentally on both ADN-rich and AN-rich sides of the diagram are in excellent agreement with the calculated liquidus straight lines. Yet, calculated eutectic points are underestimated (~ 3.5 ° C difference), whereas the eutectic composition as deduced from energy considerations made above is shifted toward higher ADN molar fraction, from x_{ADN} = 0.43 to x_{ADN} = 0.60.

DOI: 10.13009/EUCASS2017-502

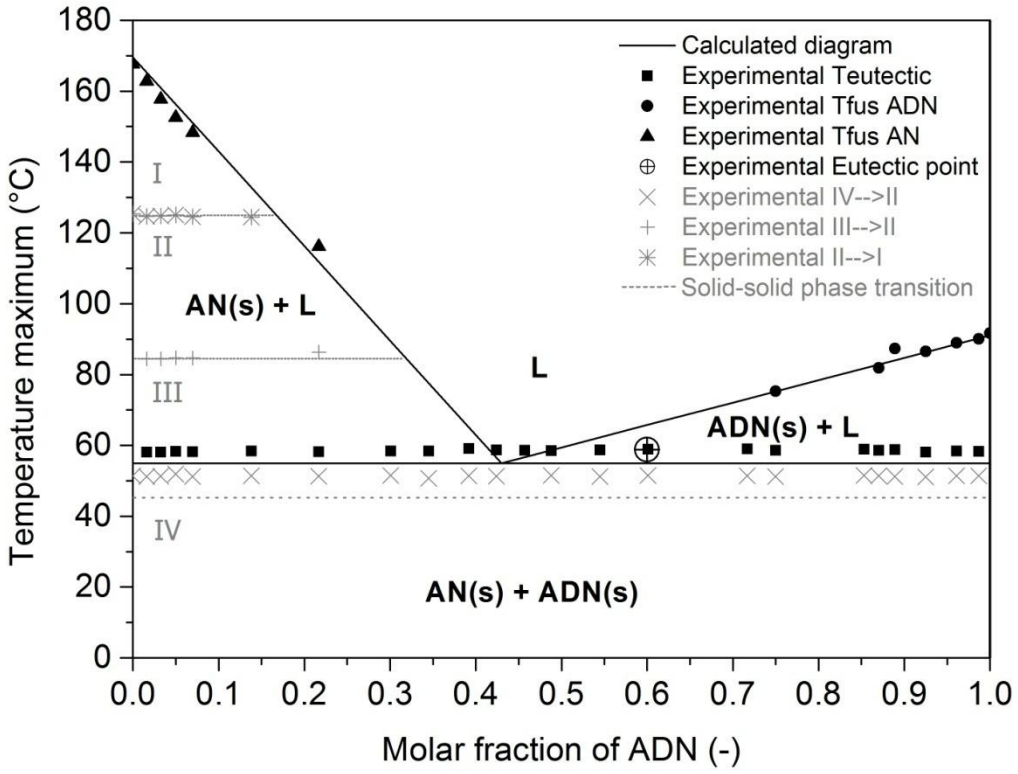

Figure 11: Experimental (with T_{max}) and calculated binary diagram

5. Conclusion

In the case of ADN-AN mixture, the equation used to the calculate the freezing point depression allowed to propose an approximate binary solid-liquid phase diagram. It is close to the experimental measurements, in particular, and surprisingly, when using the T_{max} value of the liquidus endotherm, whereas the more conventional T_{onset} was used for the determination of the eutectic temperature value. However, the calculated eutectic point seems to be slightly underestimated with this calculation method. The experimental measurement seems to show that the eutectic point is at 56.6 °C and x_{ADN}= 0.6. Experimental measurements have to be performed to confirm the binary diagram of the AN-AP mixture (Eutectic point : 166.4 °C and x_{AP} = 0.01) as well as for the ADN-AP binary system.

6. Acknowledgment

The GRAIL project has received funding from the European Union's Horizon 2020 research and innovation programme under grant agreement No 638719.

References

[1] http://grail-h2020.eu/
[2] Rahm, M. 2010. Green propellants. PhD Thesis. KTH chemical science and engineering.
[3] Pavlov, A. N., Grebennikov, V. N., Nazina, L. D., Nazia G. M. and G. B. Manelis. 1999. Thermal decomposition of ammonium dinitramide and mechanism of anomalous decay of dinitramide salts. *Russ. Chem. Bull*. 48: 50-54.
[4] Russel, T., P., Piermarini, G. J., Block, S. and P. J. Miller. 1996. Pressure, Temperature Reaction Phase Diagram for Ammonium Dinitramide. *J. Phys. Chem*. 100 : 3248-3251.

DOI: 10.13009/EUCASS2017-502

[5] Ziru, L., Yang, L., Cuimei, Y., Fengqi, Z., Yanghui, K., Yaping, Q., and P. Zhang. 1999. Thermal behavior of a new energetic material ammonium dinitramide. *Proc. Int. Pyro. Seminar*. 26:326-33.
[6] Atkins, W. 1990. Physical chemistry. Fourth edition p 179.
[7] Winborg, N., and M. Van Zelst. 2000. Comparative study of the properties of ADN and HNF. Report No. FOA-R-00-1423-310-SE.
[8] Hazards of Chemical Rockets and Propellants Handbook, Vol. 2, solid Rocket Propellant Processing, Handling, Storage and Transportation. 1972. National Technical Information Services, US department of Commerce.
[9] Kishore, K., and K. Sridhara. 1999. Condensed Phase behaviour of Ammonium Perchlorate-Based Solid Propellants. Defence research and development organization ministry of defence. New Delhi.
[10] Engel, W., and K. Menke. 1996. Development of propellants containing ammonium nitrate. *Def. Sci. J*. 46:311-318.
[11] Löbbecke, S., Keicher, T., Krause, H., and A. Pfeil. 1997. The new energetic material ammonium dinitramide and its thermal decomposition. *Solid State Ionics*. 101-103: 945-951.
[12] Keenan, A. G. 1956. The Cryoscopic Heat of Fusion of Ammonium Nitrate. *J. Phys. Chem.* 60: 1356-1361.